Supporting Information

Exploiting radical-pair intersystem crossing for maximizing singlet oxygen quantum yields in pure organic fluorescent photosensitizer

Xuanhang Wang, Yucong Song, Guocui Pan, Wenkun Han, Boyu Wang, Li Cui, Huili Ma, Zhongfu An, Zhigang Xie,* Bin Xu* and Wenjing Tian

Table of Contents

Materials and instrumentation

^{1}H NMR spectra were recorded on a 500 MHz BrukerAvance in $CDCl_3$ solutions, using $CDCl_3$ as solvent and tetramethylsilane (TMS) as an internal standard (δ = 0.00 ppm).^{13}C NMR spectra were recorded on a 125 MHz BrukerAvance, using $CDCl_3$ as a solvent and an internal standard (δ = 77.00 ppm). The time of flight mass spectra was recorded using a Kratos MALDI-TOF mass system. UV-Vis spectra were measured on a Shimadzu UV-2550 spectrophotometer. Fluorescence spectra were recorded by Shimadzu RF-5301 PC spectrometer and Maya2000Pro optical fiber spectrophotometer. The absolute fluorescence quantum yields of solutions and NPs were measured on an Edinburgh FLS920 spectrometer combined with a calibrated integrating sphere. Fluorescence lifetime and steady state spectroscopy were performed using time-correlated single-photon counting (TCSPC) method and collected on an Edinburgh FLS980, with an Edinburgh EPL-375 picosecond pulsed diode laser as the excitation source. DLS measurement was performed using a Malvern ZetasizerNano ZS size analyser at room temperature. Transmission Electron Microscopy (TEM) images were captured with a JEM-2100F instrument at a 200 kV accelerating voltage. Femtosecond transient absorption spectra were measured by ultrafast systems' Helios and Eos transient absorption spectrometers. The time resolution is ultimately limited by the pulse duration and the smallest step-size allowed by the mechanical delay line (with 8 ns time-range, 14 fs). Electrochemical measurements were performed with a BAS 100 W Bioanalytical electrochemical work station, using a glassy carbon as the working electrode, a platinum wire as the counter electrode, and a Ag/Ag^+ electrode as the reference electrode. A 0.1 M solution of n-Bu_4NPF_6 in dry CH_2Cl_2 (for oxidation) was used as the supporting electrolyte. The scan rate of the electrochemical measurements was 100 mV/s. All cyclic voltammetry graphs show voltages versus the ferrocene/ferrocenium couple. Spectroelectrochemical measurements were performed in cyclic voltammetry system with a constant voltage, and the spectral changes were recorded in a Shimadzu UV-2550 spectrophotometer.

All the other materials for organic synthesis and solvents are purchased from Sigma-Aldrich. Tetrahydrofuran (THF), toluene and 1,4-dioxane were distilled in the presence of sodium benzophenoneketyl, calcium hydride and magnesium respectively, then stored under nitrogen immediately prior to use. Dimethylformamide (DMF) was distilled and dried over potassium hydroxide.

Measure methods

Preparation of nanoparticles. The THF mixture (1mL) containing PSs (1 mg) and Pluronic F127 (10 mg) was added into 10-fold volume of water with a pipette. The THF/water mixture was then sonicated for 5 min in a microtip ultrasound sonicator (Bransonic, MH 2510). The residual THF in the solution was removed by stirring in fume hood overnight. The NPs was obtained by filtering with a 0.4 μm syringe driven filter.

Singlet oxygen quantum yield measurements *via* chemical method. 9,10-anthracenediylbis(methylene)dimalonic acid (ABDA) was used as $^1O_2$-trapping agent

to specifically detect singlet oxygen production. The mixture dissolving ABDA (100 μM) and different PSs (10 μM) was exposed to white light irradiation (400-800 nm). The absorbance decrease of ABDA at 400 nm was recorded by Shimadzu UV-2550 spectrophotometer at various irradiation times. The $^1O_2$ quantum yield (Φ_O) of the PSs was obtained by the following calculation formula:

$$\Phi_O = \Phi_{RB} * K_{PS} * A_{RB} / (K_{RB} * A_{PS})$$

Rose Bengal (RB) serves as the standard photosensitizer and Φ_{RB} is the singlet oxygen quantum yield of RB (75%) in water. K_{PS} and K_{RB} are the absorbance decomposition rate of ABDA at 400 nm in the presence of PSs and RB. A_{PS} and A_{RB} represent the integration of the UV-visible absorption bands covering the wavelength range of 400-700 nm of PSs and RB.

Density functional theory calculations. All the calculations were performed phase using a Gaussian 09 program. The ground state of all molecules was fully optimized by the hybrid B3LYP, in combination with 6-31G (d, p) basis set. The excited-state characteristics were calculated by the time-dependent density functional theory (TD-DFT).

Cell culture. HeLa cells (human cervical cancer cell line) were purchased from Jilin University and grown in Dulbecco's modified Eagle's medium (DMEM, GIBCO), which was supplemented with 10% heat-inactivated fetal bovine serum (FBS, GIBCO), 100 U/mL penicillin and 100 μg/mL streptomycin (Sigma). The temperature of the incubator is maintained at 37 °C, with 5% CO_2.

Co-localization of lysosome and NPs. HeLa cells were incubated with NPs (10 μg/mL) for 6 h. The supernatant was then removed and the washed cells with phosphate buffer saline (PBS). Soon after, Cells were immersed into each well containing 4% formaldehyde (1 mL) at room temperature. The cells were washed twice with PBS after ten min, and then stained with Lyso-Tracker Green for 1 h. The cells were washed twice with PBS again and cell nuclei were stained with DAPI. Finally, the images of cells were examined by CLSM.

Cytotoxicity assay. HeLa cells were harvested during the logarithmic growth phase and seeded into 96-well plates at a density of 10^4 cells per well and incubated for 24 h. The NPs with different concentration gradients (0-4 μg/mL for PTP NPs, 0-10 μg/mL for TP NPs) were added to the cell culture medium separately and incubated with the cells for 6 h. The light group received irradiation (450 nm, 20 mW/cm^2) for 40 min and the dark control group received nothing, and continued incubation for 24 h in the same environment. MTT (20 μL) was then added to the medium and incubated for 4 h. The absorbance of MTT at 490 nm was measured by Bio-Rad 680 microplate reader.

Live / dead cell staining assay. HeLa cells were harvested in a logarithmic growth phase and seeded into 96-well plates at a density of 10^4 cells per well and incubated for 24 h. The NPs (10 μg/mL) were added to the cell culture medium and incubated with the cells for 6 h. The light group received irradiation (450nm, 20mW/cm^2) for 30 min and then continued to incubate for 24 h. The dark control group received nothing and incubated for the same time as the light group. The cells were stained with Calcein-AM/PI for 40 min and were then washed with PBS. Finally, the images of cells were observed through a Nikon C1si laser scanning confocal microscopy.

Intracellular ROS assays. HeLa cells were seeded in 6-well culture plates at a density of 5×10^4 cells per well for 24 h. Then the NPs (20 μg/mL) were added into cell culture medium separately. After incubated for 6 h, the light group received irradiation (450nm, 20 mW/cm^2) for 20 min, the dark control group received nothing. Then using the DMEM solution washed cells. The DMEM solution containing DCFH-DA (10 μmol/L) was added and incubated for 30 min. The cells were observed by CLSM with the excitation at 488 nm.

Animal experiments. All animal studies were performed in strict accordance with the NIH guidelines for the care and use of laboratory animals (NIH Publication No. 85-23 Rev.1985) and was approved by the guidelines of the Committee on Animal Use and Care of Chinese Academy of Sciences. Male mice were purchased from Jilin University, China (6 weeks, 15-20 g). The tumor-bearing mouse models were established by inoculating the subcutaneous murine U14 Cervical cancer cells (100 μL) into the right thigh.

***In vivo* PDT.** One week later, the mice were injected with PTP NPs (100 μg/mL, 100 μL) intravenously, and the control group received normal saline. After 1 h, the tumor site of the mouse was then irradiated with laser light (450 nm, 200 mW/cm^2) for 20 min per day. The tumor volume and body weight of the mice were measured per three days for 15 days. Histological analysis: The mice were sacrificed on day 15 and tumors were collected and fixed in 4% paraformaldehyde. They were then embedded in paraffin and sliced at thickness of 5 μm. Slices were stained with hematoxylin and eosin (H&E) and imaged by optical microscopy.

Supplementary Figures

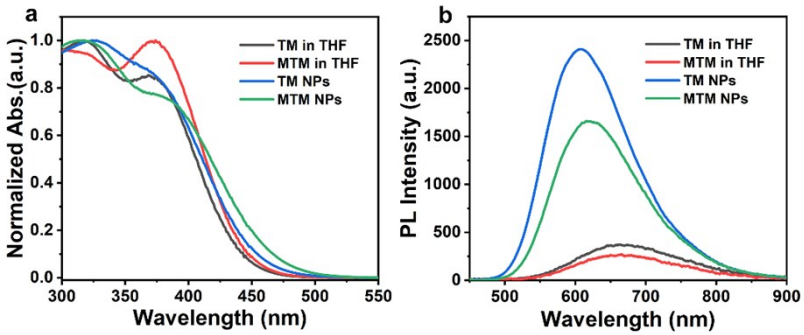

Figure S1. (a) UV-visible absorption spectrum of TM and MTM in THF and NPs aqueous solution. (b) PL spectra of TM and MTM in THF and NPs aqueous solution.

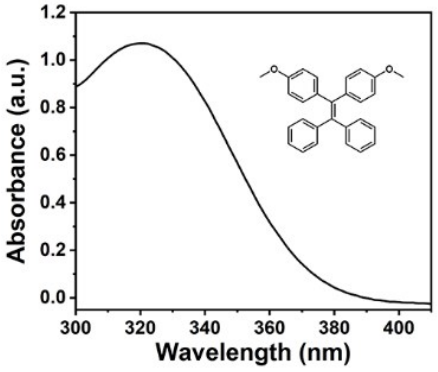

Figure S2. UV-visible absorption spectrum of TPE in THF.

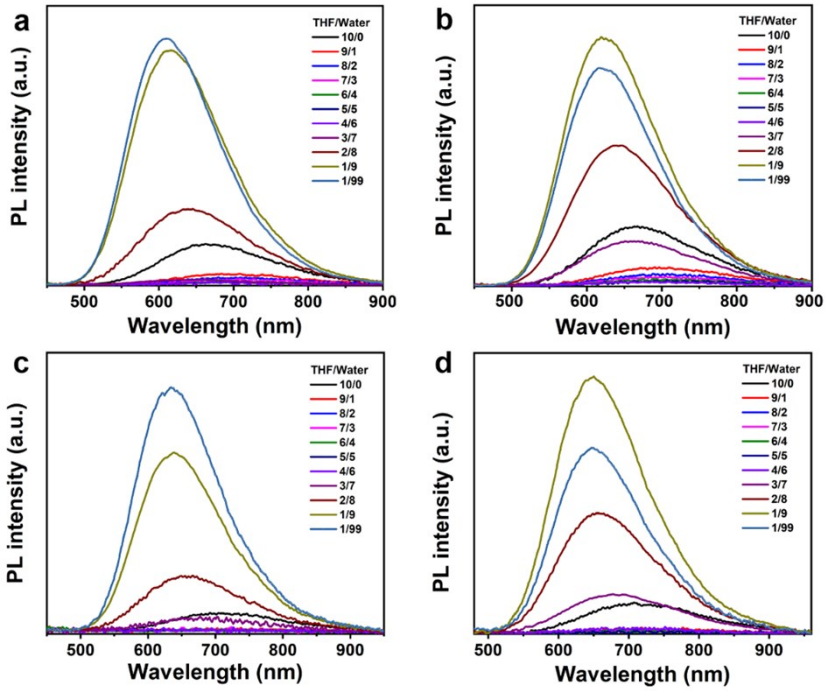

Figure S3. PL spectra of TM (a), MTM (b), TP (c) and PTP (d) in THF-water mixtures at different volume ratios.

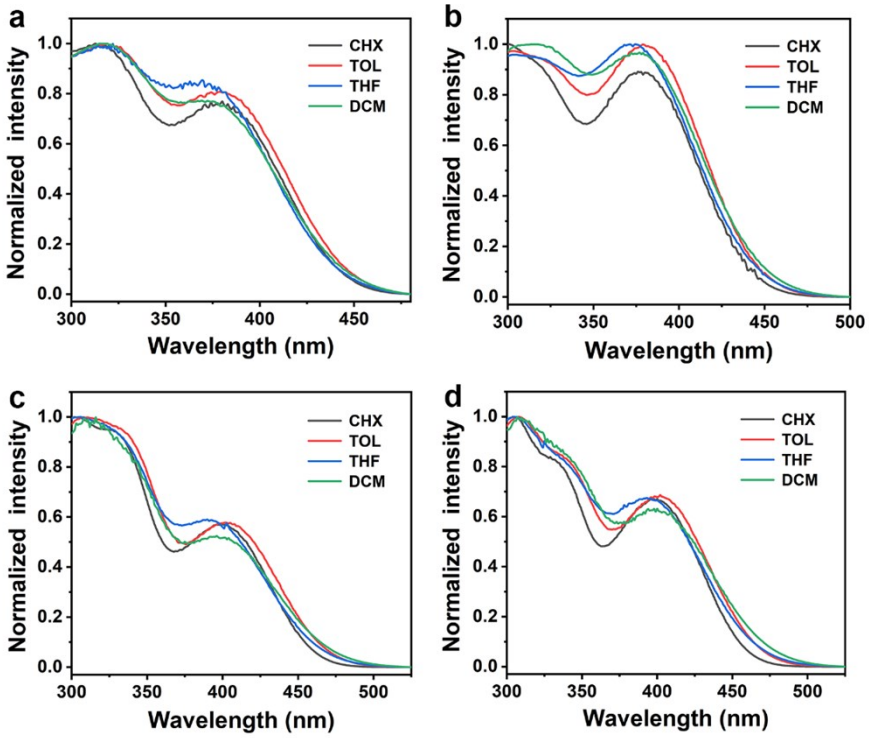

Figure S4. UV-visible absorption spectrum of TM (a), MTM (b), TP (c) and PTP (d) in different polar solvents. The abbreviations of solvent are as follows: cyclohexane (CHX), toluene (TOL), tetrahydrofuran (THF), dichloromethane (DCM).

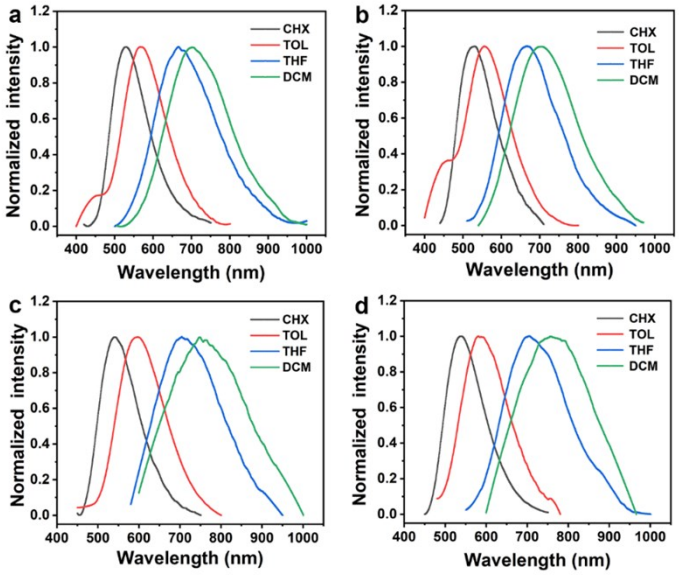

Figure S5. PL spectra of TM (a), MTM (b), TP (c) and PTP (d) in different polar solvents.

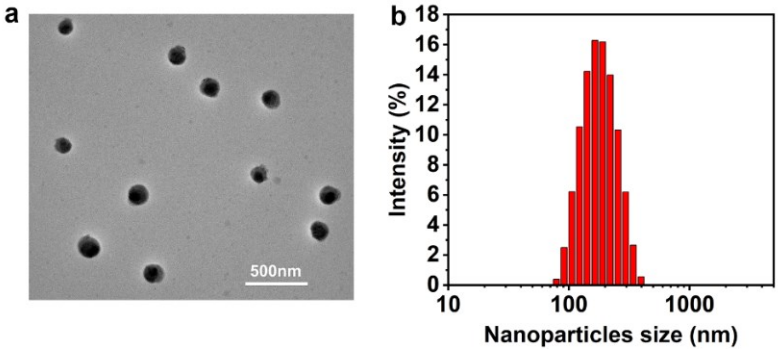

Figure S6. The TEM image (a) and the dynamic laser scattering results (b) of PTP NPs.

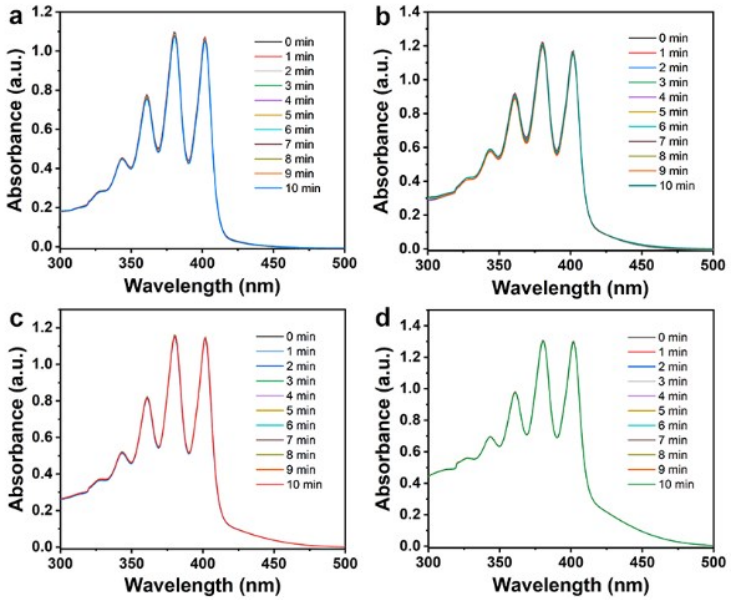

Figure S7. UV-visible spectra of ABDA in the presence of TM (a), MTM (b), TP (c)

and PTP (d) in N, N-dimethylformamide (DMF) solution under light irradiation (400-800 nm) for different time. [PSs] = 10 μM, [ABDA] = 100 μM.

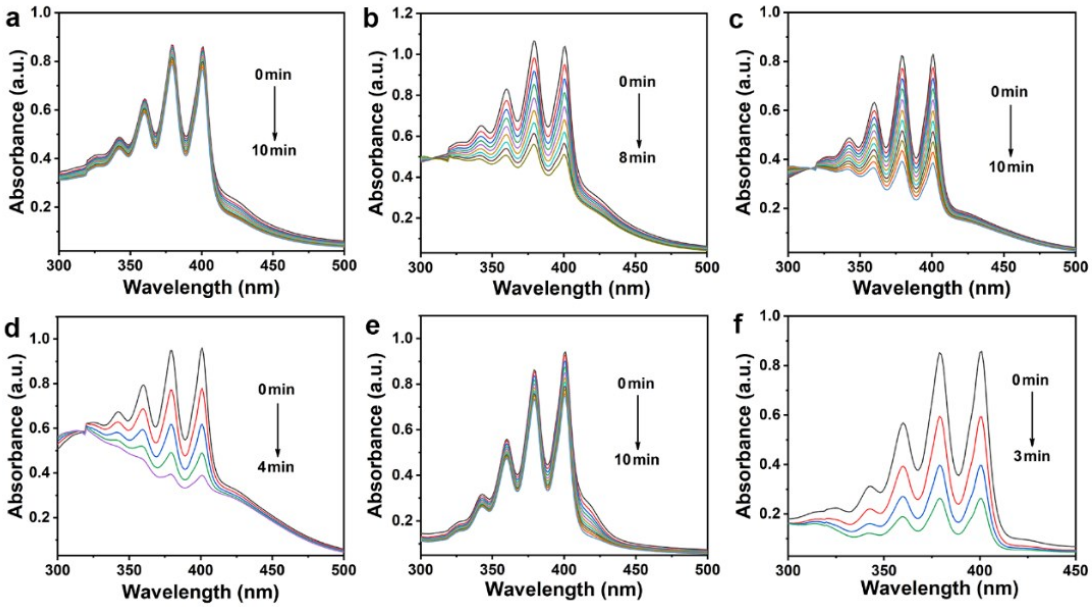

Figure S8. UV-visible spectra of ABDA in the presence of TM NPs (a), MTM NPs (b), TP NPs (c), PTP NPs (d), Ce6 (e) and RB (f) under light irradiation (400-800 nm) for different time. [PSs] = 10 μM, [ABDA] = 100 μM.

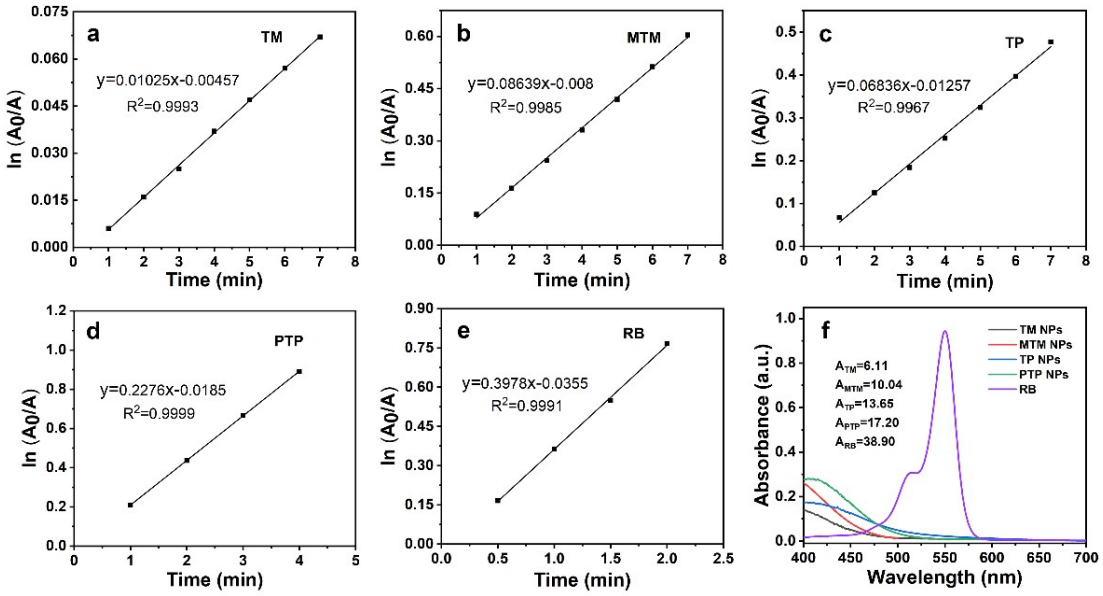

Figure S9. Decomposition rate constants of ABDA with TM NPs (a), MTM NPs (b), TP NPs (c), PTP NPs (d) and RB (e), respectively. (f) The integration of the absorption bands of TM NPs, MTM NPs, TP NPs, PTP NPs and RB in the wavelength range of 400-700 nm.

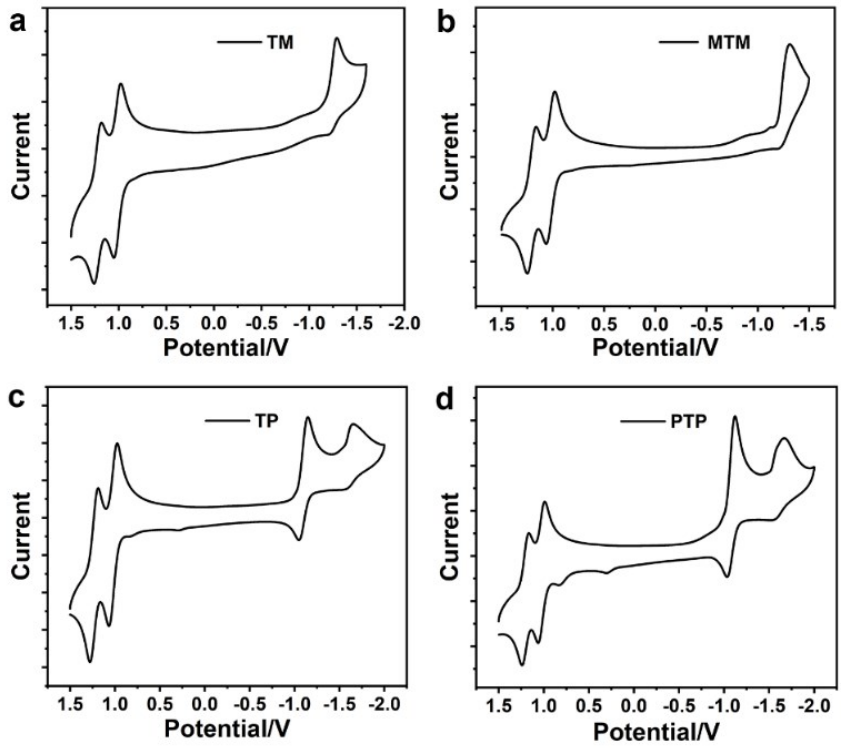

Figure S10. Cyclic voltammogram of TM (a), MTM (b), TP (c) and PTP (d). Ferrocene (Fc) was used as internal reference in deaerated THF, n-Bu_4NPF_6 as supporting electrolyte.

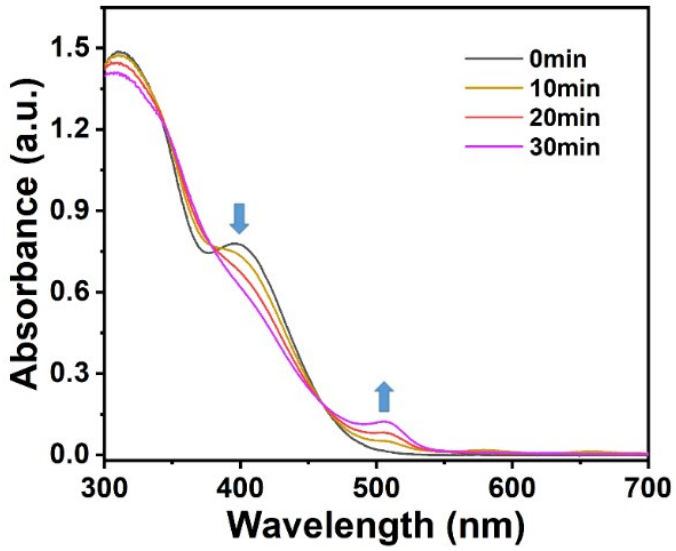

Figure S11. Spectral changes observed upon controlled-potential, bulk electrolysis of TP at -1.5 V in a 0.1 M n-Bu_4NPF_6 solution in dichloromethane.

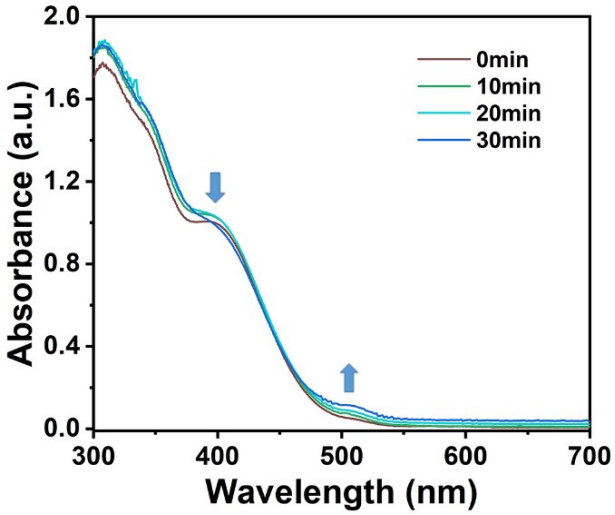

Figure S12. Spectral changes observed upon controlled-potential, bulk electrolysis of PTP at -1.5 V in a 0.1 M n-Bu_4NPF_6 solution in dichloromethane.

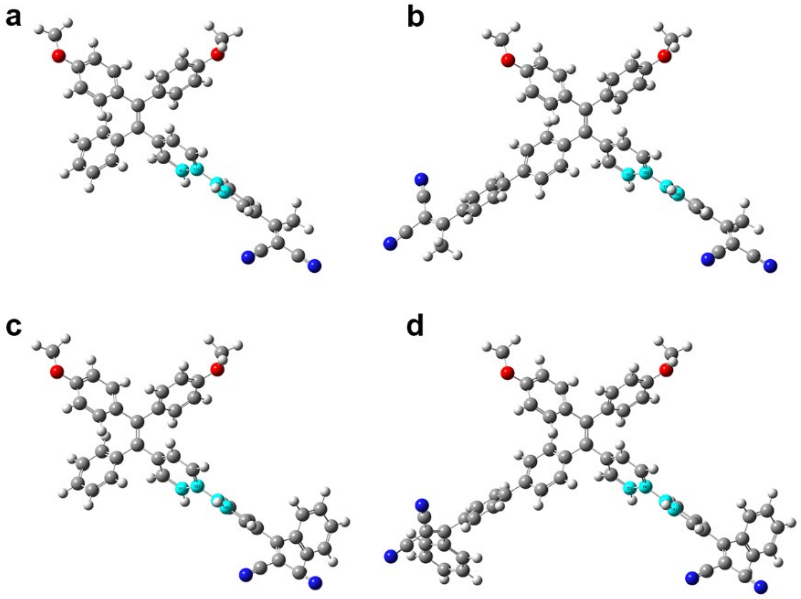

Figure S13. Geometry configurations of TM (a), MTM (b), TP (c) and PTP (d) were fully optimized by the hybrid B3LYP, in combination with 6-31G (d, p) basis set.

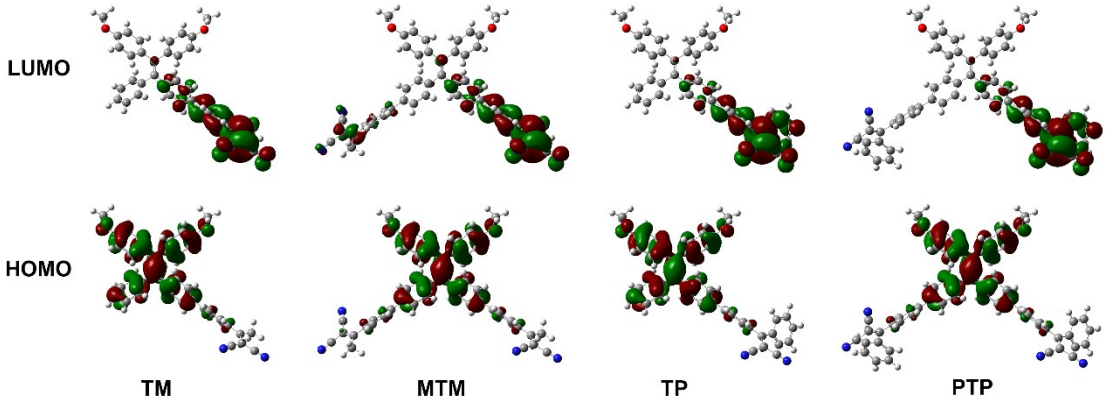

Figure S14. The HOMO-LUMO distribution of TM, MTM, TP and PTP.

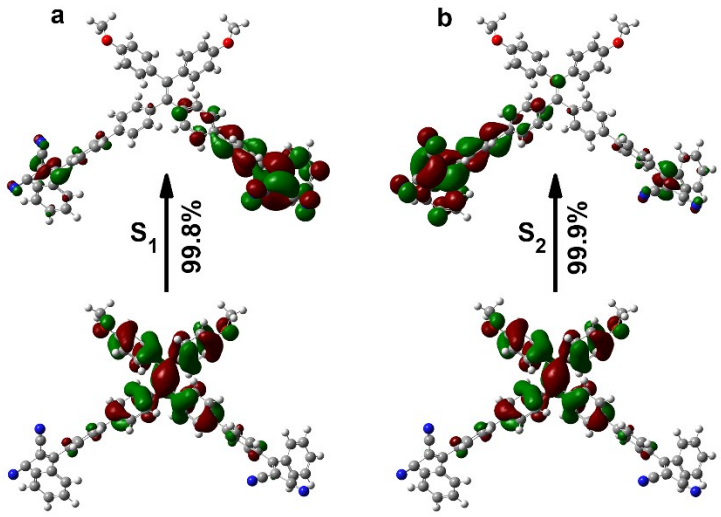

Figure S15. The natural transition orbitals (hole ones at the bottom and electron ones on the top) for S_1(a) and S_2 (b) of PTP.

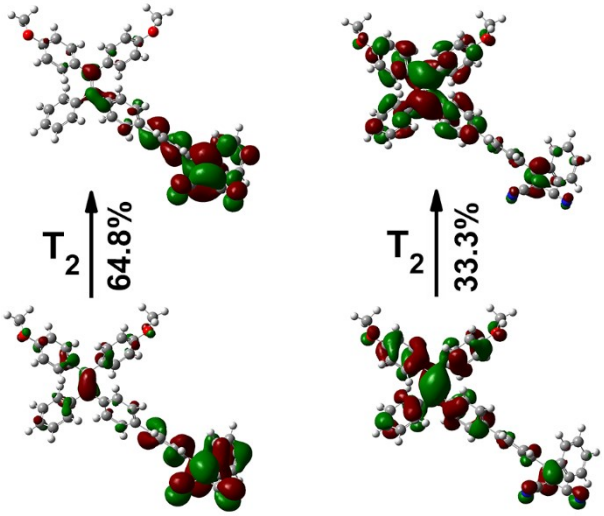

Figure S16. The natural transition orbitals for T_2 of TP.

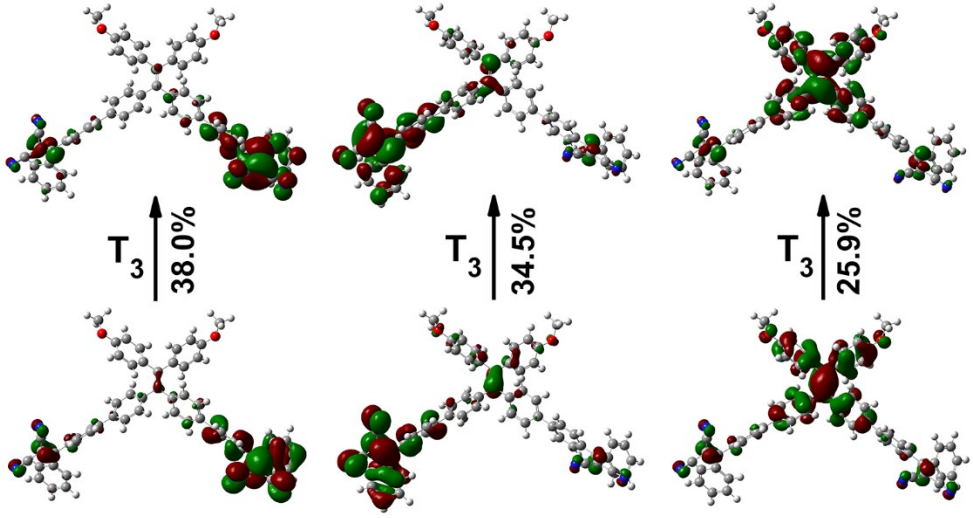

Figure S17. The natural transition orbitals for T_3 of PTP.

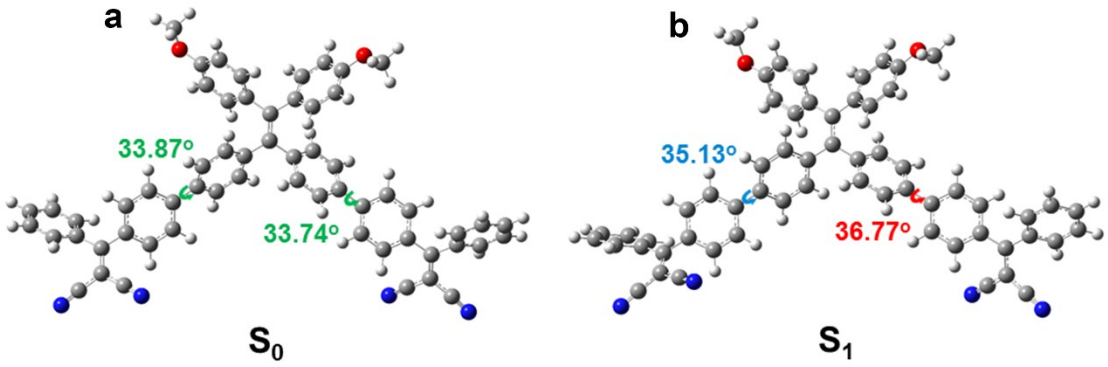

Figure S18. Comparison between the S_0 (a) and S_1 (b) optimized geometries of PTP.

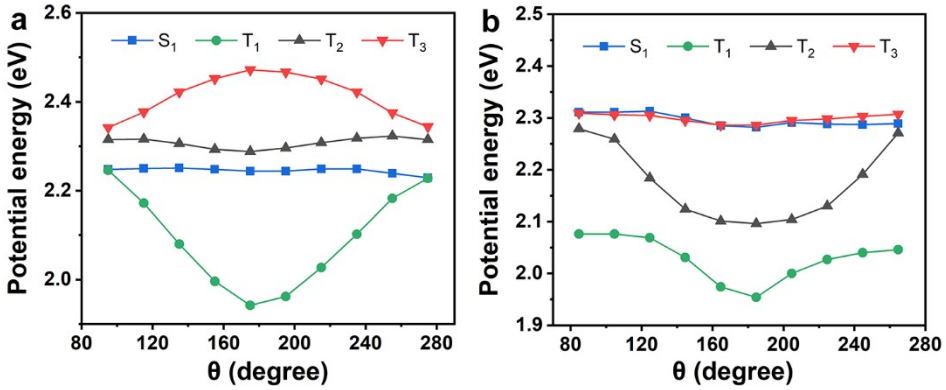

Figure S19. The potential energy curves of S_1, T_1, T_2, and T_3 states for asymmetric molecule TP (a) and symmetric molecule PTP (b) calculated by the TDDFT/B3YLP/6-31G (d, p) method (θ represents the dihedral angle of donor-acceptor).

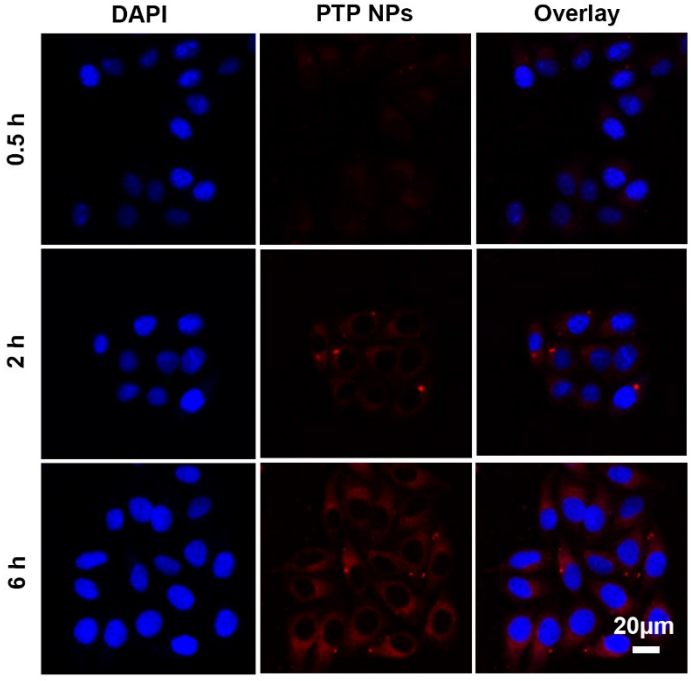

Figure S20. Fluorescence and merged images of HeLa cells at different incubated time.

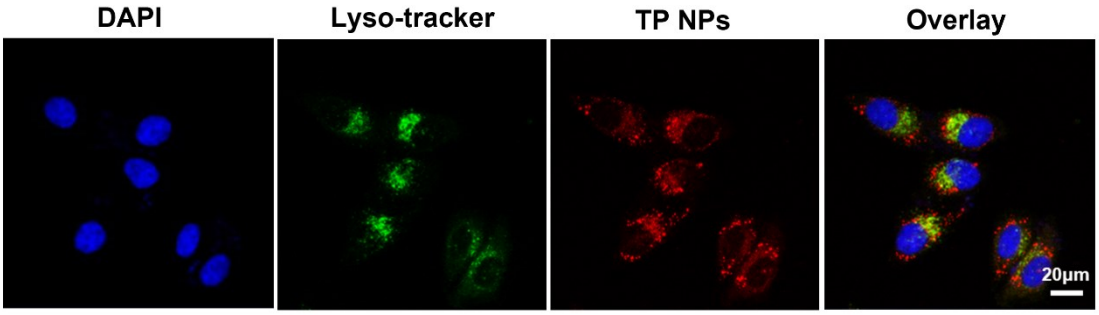

Figure S21. Confocal and merged images of HeLa cells stained with DAPI, Lyso-tracker and TP NPs, Excitation: 488 nm.

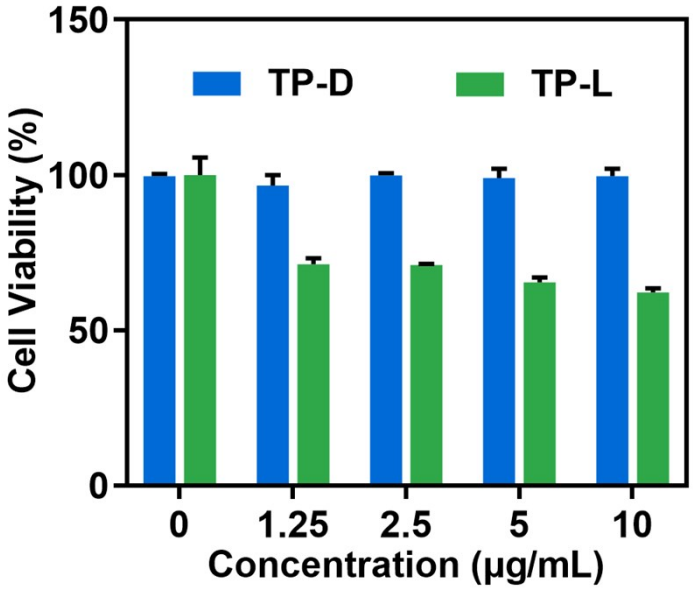

Figure S22. Cell viability of HeLa cells treated with TP NPs of different concentrations under light irradiation or dark conditions.

Supplementary Tables

Table S1. Photophysical data of TM, MTM, TP and PTP in toluene and aqueous solution.

	Φ_{QY}(%)		τ(ns)		k_r (x10^7 s^{-1})		k_{nr} (x10^8 s^{-1})	
	Tol	NPs	Tol	NPs	Tol	NPs	Tol	NPs
TM	1.71	12.35	0.73	8.28	2.34	1.49	13.46	1.06
MTM	1.21	5.98	0.86	5.85	1.41	1.02	11.49	1.61
TP	4.62	11.22	0.73	11.1	6.33	1.01	13.07	0.8
PTP	2.28	2.96	0.92	7.57	2.48	0.39	10.62	1.28

Table S2. Optical properties of TM, MTM, TP, PTP in different polar solvents.

	TM		MTM		TP		PTP	
	λ_{abs}(nm)	λ_{em}(nm)	λ_{abs}(nm)	λ_{em}(nm)	λ_{abs}(nm)	λ_{em}(nm)	λ_{abs}(nm)	λ_{em}(nm)
CHX	380	531	376	530	400	540	400	535
TOL	379	568	379	563	402	591	402	591
THF	370	651	374	651	390	707	393	705
DCM	369	701	377	700	396	737	400	738

Table S3. The energy of HOMO and LUMO of TM, MTM, TP and PTP.

	TM	MTM	TP	PTP
LUMO (eV)	-3.19	-3.17	-3.32	-3.36
HOMO (eV)	-5.29	-5.31	-5.32	-5.31

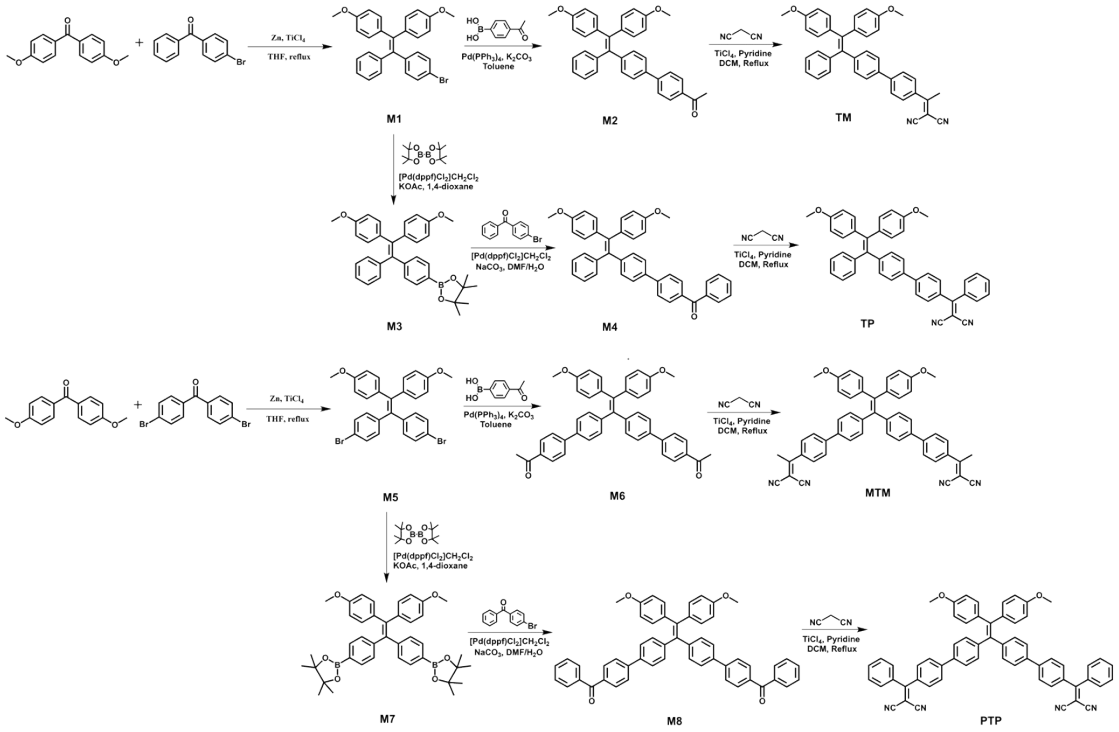

Figure S23. The synthetic route to four AIE photosensitizers.

Molecular synthesis procedure

Compounds of **TM** and **TP** have been prepared in previous work,[1] according to the synthetic route presented in Figure S23.

Synthesis of compound M5

To the solution of 4,4'-dibromobenzophenone (3 g, 8.82 mmol) and 4,4'-dimethoxybenzophenone (2.14 g, 8.83 mmol) in dry THF (100 mL) was added zinc powder (6.18 g, 95.1 mmol). Then the suspension was cooled down to -78 ^{o}C. Titanium tetrachloride (5.22 mL, 47.50 mmol) was added to the above mixture dropwise. After addition, the mixture was slowly warmed up to room temperature, followed by refluxing for 8 hours. Then the mixture was cooled down in ice-water bath and saturated

sodium bicarbonate aqueous solution (50 mL) was added slowly. The mixture was extracted with ethyl acetate (100 mL × 3). The combined organic phase was washed with brine (100 mL × 2) and dried over Na_2SO_4. Then the mixture was filtered and the filtrate was concentrated under reduced pressure. The desired residue was purified with chromatography (petroleum ether/dichloromethane = 4/1, v/v) to give the desired product as a white solid (2.1 g, 43.3% yield).^{1}H NMR (500 MHz, Chloroform-d), δ 7.25-7.22 (m, 4H), 6.95-6.85 (m, 8H), 6.67-6.64 (m, 4H), 3.76 (s, 6H).

Synthesis of compound M6

4-acetylphenylboronic acid (3.58 g, 21.8 mmol), **M5** (2.00 g, 3.63 mmol) and the $Pd(PPh_3)_4$ (0.42 g, 0.36 mmol) catalyst were dissolved in toluene (20.0 mL), and then 2M aqueous K_2CO_3 solution (10 mL) was added to solution. The mixture was stirred under a nitrogen atmosphere at 75 °C for 16 h. After cooling to room temperature, the mixture was extracted with ethyl acetate (50 mL × 3). The combined organic phase was washed with brine (100 mL × 2) and dried over Na_2SO_4. Then the mixture was filtered and the filtrate was concentrated under reduced pressure. The combined organic phase was concentrated and purified by silica gel column chromatography (dichloromethane /ethyl acetate = 60/1, v/v). The product was dried under vacuum to afford compound **M6** as a light yellow solid (1.7 g, 74.5% yield).^{1}H NMR (500 MHz, Chloroform-d) δ 8.02-7.97 (m, 4H), 7.69-7.64 (m, 4H), 7.44-7.40 (m, 4H), 7.17-7.13 (m, 4H), 7.02-6.98 (m, 4H), 6.70-6.65 (m, 4H), 3.75 (s, 6H), 2.62 (s, 6H).

Synthesis of compound MTM

To the solution **M6** (500 mg, 0.80 mmol) and malononitrile (263 mg, 3.98 mmol) of in dry dichloromethane (20 mL) was added titanium tetrachloride (0.52 mL, 4.73 mmol) slowly at 0 °C. After the reaction mixture was stirred for 30 min, pyridine (0.38 mL, 4.72 mmol) was injected and stirred for another 30 min. Then the mixture was heated at 40 °C for 8h. After the mixture was cooled down to room temperature, the reaction was quenched by saturated sodium bicarbonate aqueous solution (30 mL) and the mixture was extracted with ethyl acetate (50 mL × 3). The collected organic layer was washed by brine, dried over Na_2SO_4 and concentrated under reduced pressure. The desired mixture was purified by column chromatography using (dichloromethane /ethyl acetate = 60/1, v/v) as eluent to give the desired product **MTM** as a yellow solid (350 mg, 60.4%).^{1}H NMR (500 MHz, Chloroform-*d*) δ 7.70 (d, *J* = 8.4 Hz, 4H), 7.63 (d, *J* = 8.4 Hz, 4H), 7.41 (d, *J* = 8.2 Hz, 4H), 7.16 (d, *J* = 8.2 Hz, 4H), 6.99 (d, *J* = 8.6 Hz, 4H), 6.67 (d, *J* = 8.6 Hz, 4H), 3.75 (s, 6H), 2.67 (s, 6H). ^{13}C NMR (126 MHz, Chloroform-d) δ 174.55, 158.42, 144.76, 144.62, 136.68, 135.95, 134.32, 132.66, 132.17, 128.08, 127.28, 126.45, 113.20, 113.09, 112.93, 55.14, 29.71, 24.05. MS: m/z: [M+] calcd for $C_{50}H_{36}N_4O_2$: 724.28, found: 724.05.

Synthesis of compound M7

Compound **M5** (1.5 g, 2.73 mmol), bis(pinacolato)diboron (2.08 g, 8.19 mmol), potassium acetate (0.8 g, 8.19 mmol), $[Pd(dppf)Cl_2]CH_2Cl_2$ (0.33 g, 0.41 mmol) and 1,4-dioxane (40 mL) were mixed together in a 250 mL flask. After degassing, the reaction mixture was kept at 85 °C for 24h, and then cooled to room temperature. Add water to the solution and the mixture was extracted with ethyl acetate (50 mL × 3). The organic layer was separated and dried over Na_2SO_4. After removal of the solvents, the

crude product was purified on a silica gel column using dichloromethane/petroleum ether (1/1, v/v) as the eluent to afford **M7** as a white solid (1.2 g, 68.2%). ^{1}H NMR (500 MHz, Chloroform-d) δ 7.52 (d, J = 8.1 Hz, 4H), 7.00 (d, J = 8.1 Hz, 4H), 6.92 (d, J = 8.7 Hz, 4H), 6.65-6.59 (m, 4H), 3.74 (s, 6H), 1.32 (s, 24H).

Synthesis of compound M8

Compound **M7** (1 g, 1.55 mmol), 4-bromobenzophenone (1.62 g, 6.2 mmol), [Pd(dppf)Cl_2]CH_2Cl_2 (0.13 g, 0.16 mmol), DMF (20 mL) and 2M aqueous K_2CO_3 solution (10 mL) was carefully degassed and charged with nitrogen. The reaction mixture was then stirred at 60 °C for 12 h. After cooling down the reaction mixture to ambient temperature, it was extracted with ethyl acetate and washed with water. The organic layer was separated and dried over Na_2SO_4. After evaporation of the solvent, the mixture was purified by column chromatography on silica gel by using dichloromethane/petroleum ether/ ethyl acetate (10/10/1, v/v) as the eluent to afford **M8** as a yellow-green solid (0.83 g, 71.1% yield). ^{1}H NMR (500 MHz, Chloroform-d) δ 7.86 (d, J = 8.2 Hz, 4H), 7.82 (dt, J = 7.3, 1.3 Hz, 4H), 7.70-7.67 (m, 4H), 7.61-7.57 (m, 2H), 7.49 (t, J = 7.6 Hz, 4H), 7.45 (d, J = 8.2 Hz, 4H), 7.17 (d, J = 8.1 Hz, 4H), 7.01 (dd, J = 8.4, 1.3 Hz, 4H), 6.70-6.66 (m, 4H), 3.75 (s, 6H).

Synthesis of compound PTP

To the solution **M8** (400 mg, 0.53 mmol) and malononitrile (211 mg, 3.19 mmol) of in dichloromethane (20 mL) was added titanium tetrachloride (0.35 mL, 3.18 mmol) slowly at 0 °C. After the reaction mixture was stirred for 30 min, pyridine (0.26 mL, 3.18 mmol) was injected and stirred for another 30 min. Then the mixture was heated at 40 °C for 8h. After the mixture was cooled down to room temperature, the reaction was quenched by saturated sodium bicarbonate aqueous solution (30 mL) and the mixture was extracted with ethyl acetate (50 mL × 3). The collected organic layer was washed by brine, dried over Na_2SO_4 and concentrated under reduced pressure. The desired mixture was purified by column chromatography using dichloromethane/petroleum ether/ethyl acetate (20/10/1, v/v) as eluent to give the desired product **PTP** as an orange solid (280 mg, 62.3% yield). ^{1}H NMR (500 MHz, Chloroform-d) δ 7.67 (d, J = 8.3 Hz, 4H), 7.59 (t, J = 7.2 Hz, 2H), 7.53-7.48 (m, 8H), 7.46 (d, J = 7.8 Hz, 4H), 7.42 (d, J = 8.1 Hz, 4H), 7.15 (d, J = 8.1 Hz, 4H), 6.99 (d, J = 8.6 Hz, 4H), 6.67 (d, J = 8.6 Hz, 4H), 3.75 (s, 6H). ^{13}C NMR (126 MHz, Chloroform-d) δ 174.44, 158.42, 145.09, 144.69, 136.69, 136.12, 135.94, 134.56, 132.65, 132.18, 131.15, 130.50, 128.87, 127.02, 126.51, 114.14, 113.20, 55.14. MS: m/z: [M+] calcd for $C_{60}H_{40}N_4O_2$: 848.32, found: 847.95.

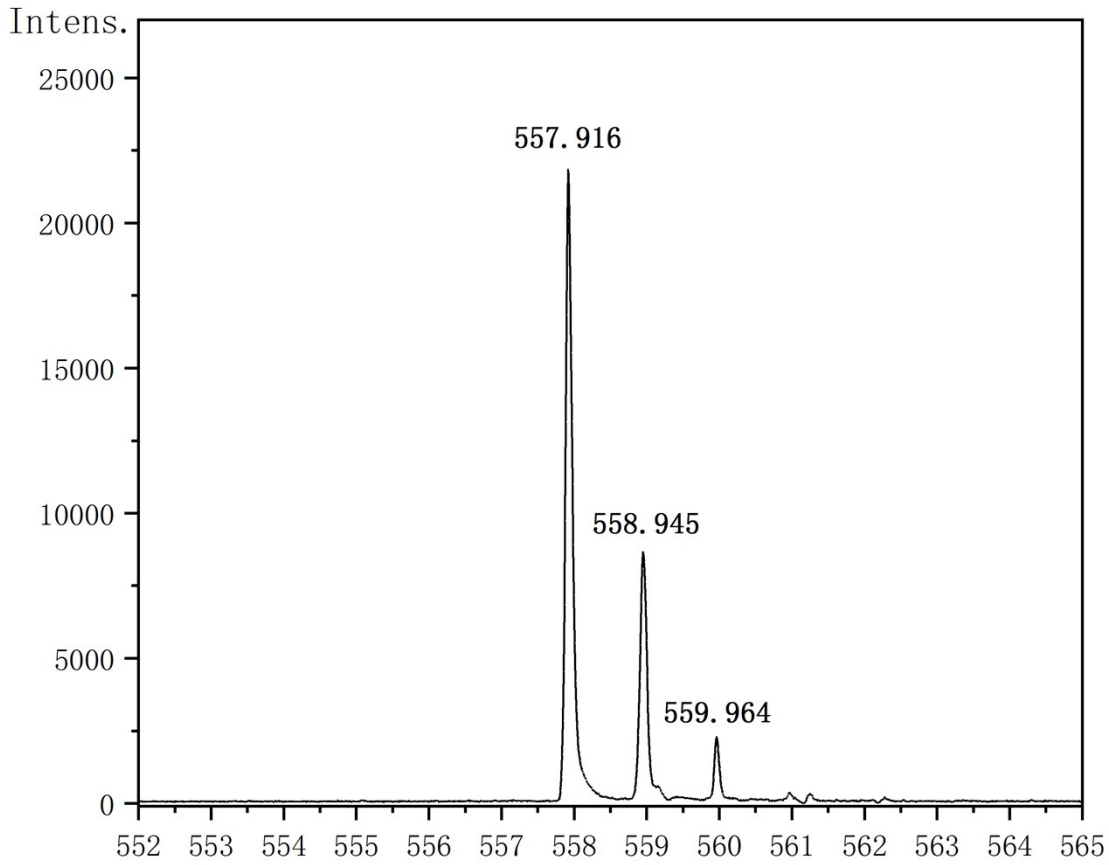

Figure S24. The MALDI-TOF mass spectrum of TM.

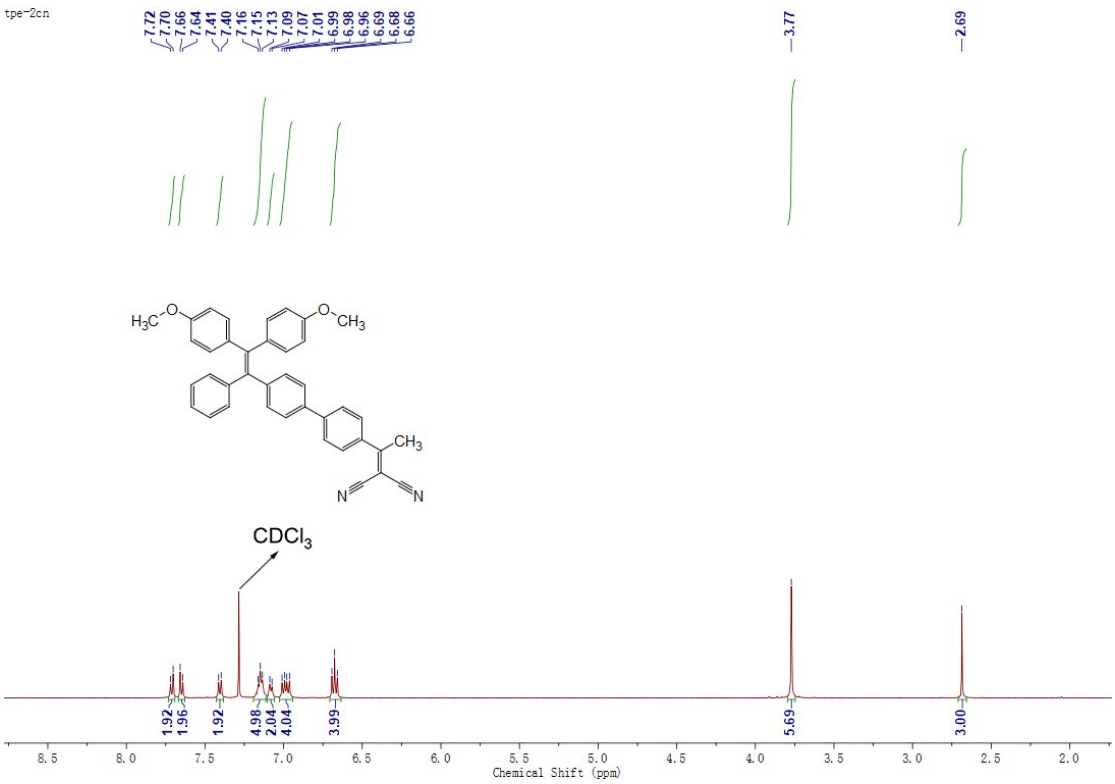

Figure S25. ^{1}H NMR spectrum of TM in chloroform-d.

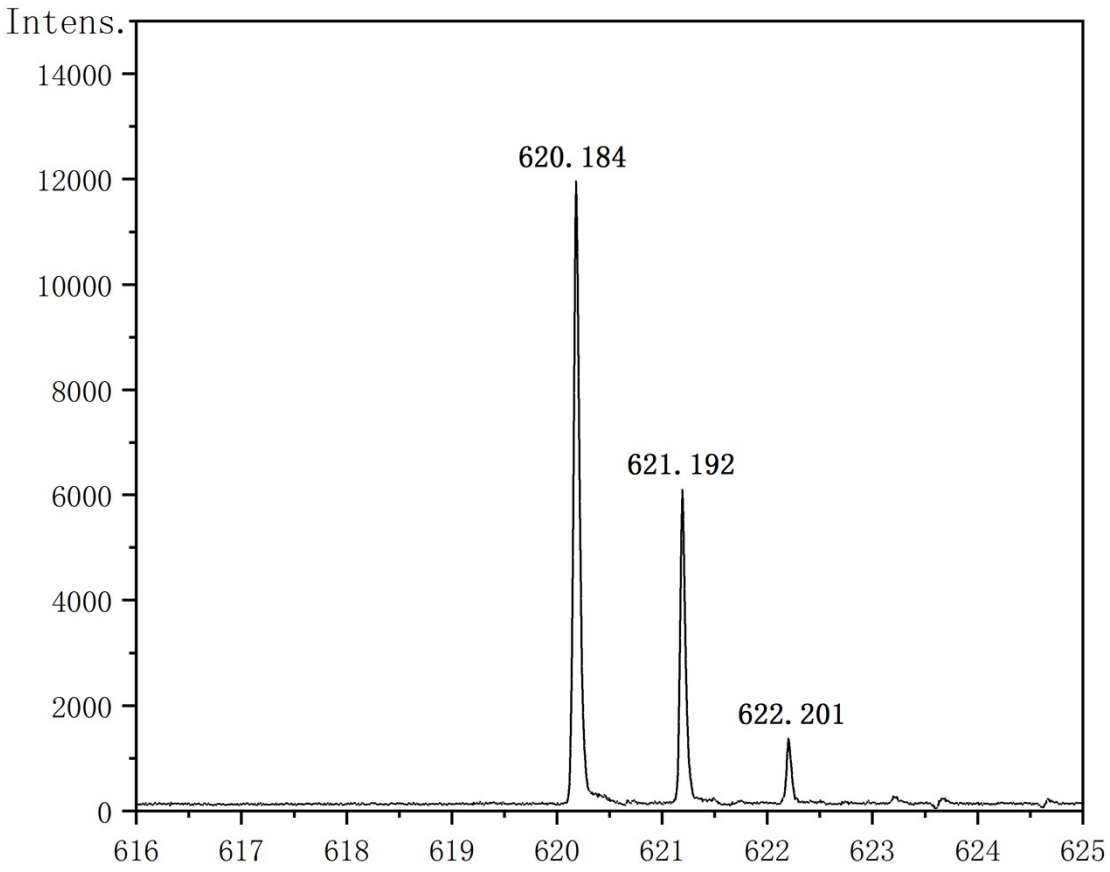

Figure S26. The MALDI-TOF mass spectrum of TP.

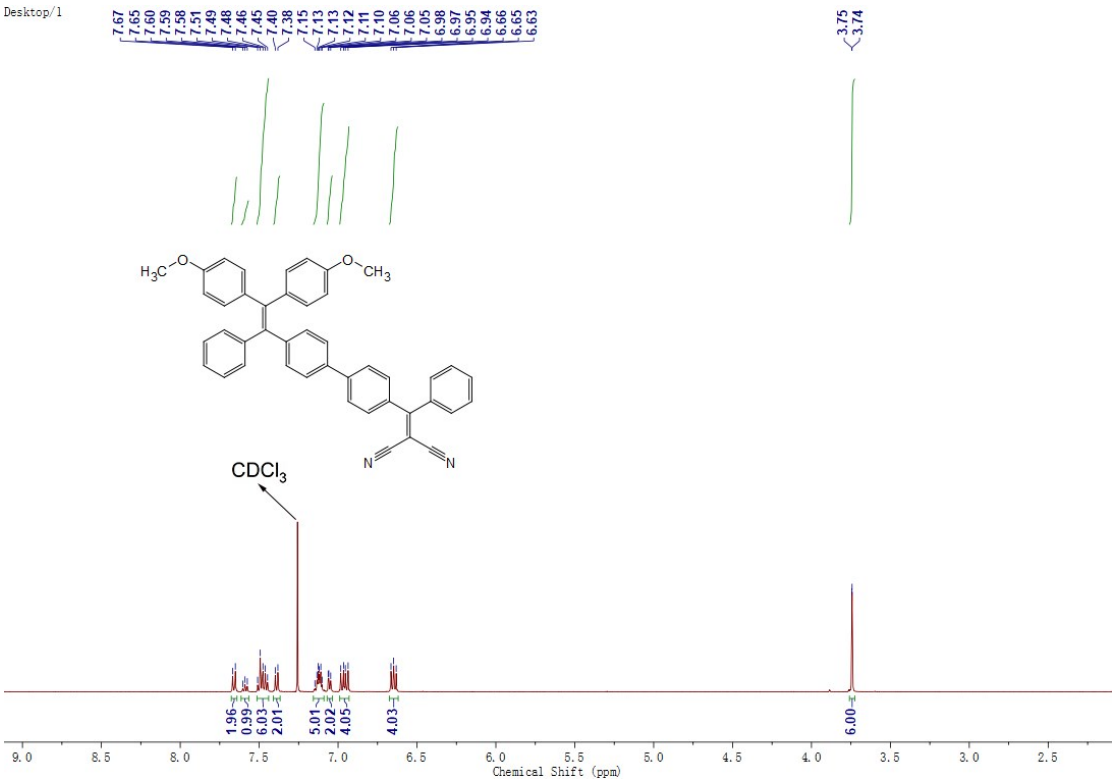

Figure S27. ^{1}H NMR spectrum of TP in chloroform-d.

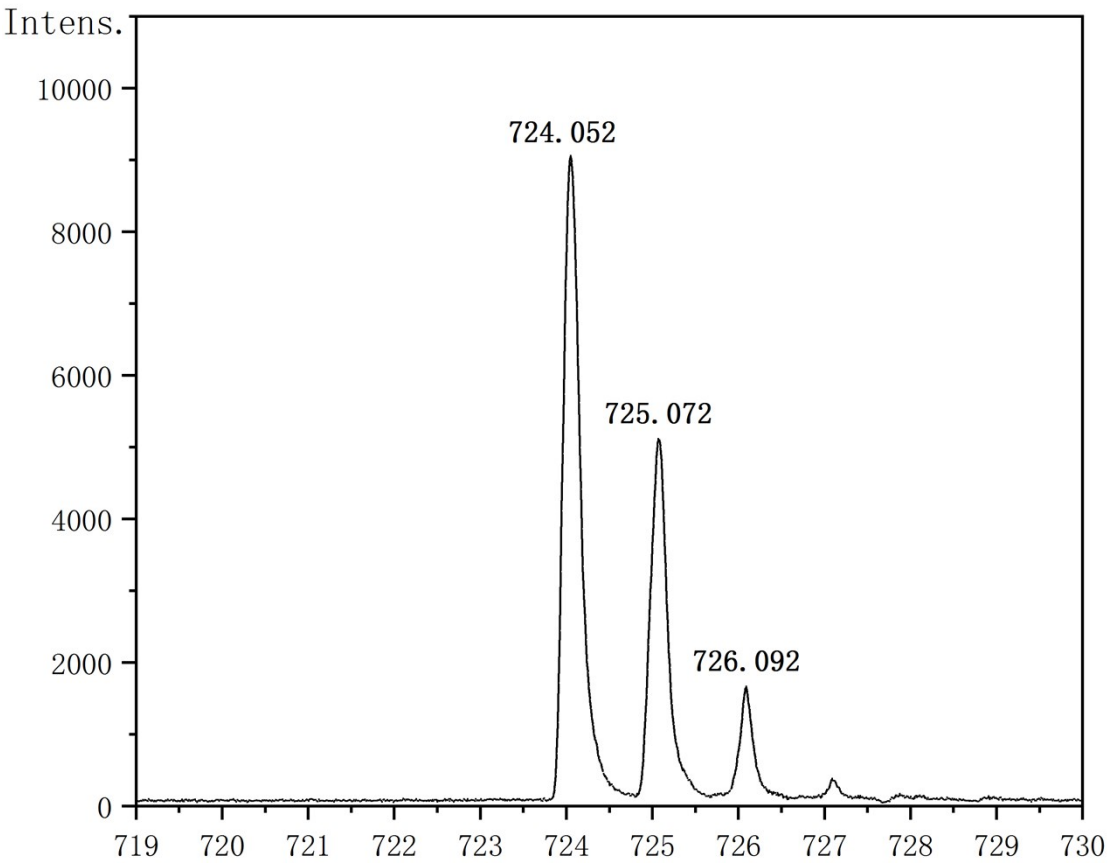

Figure S28. The MALDI-TOF mass spectrum of MTM.

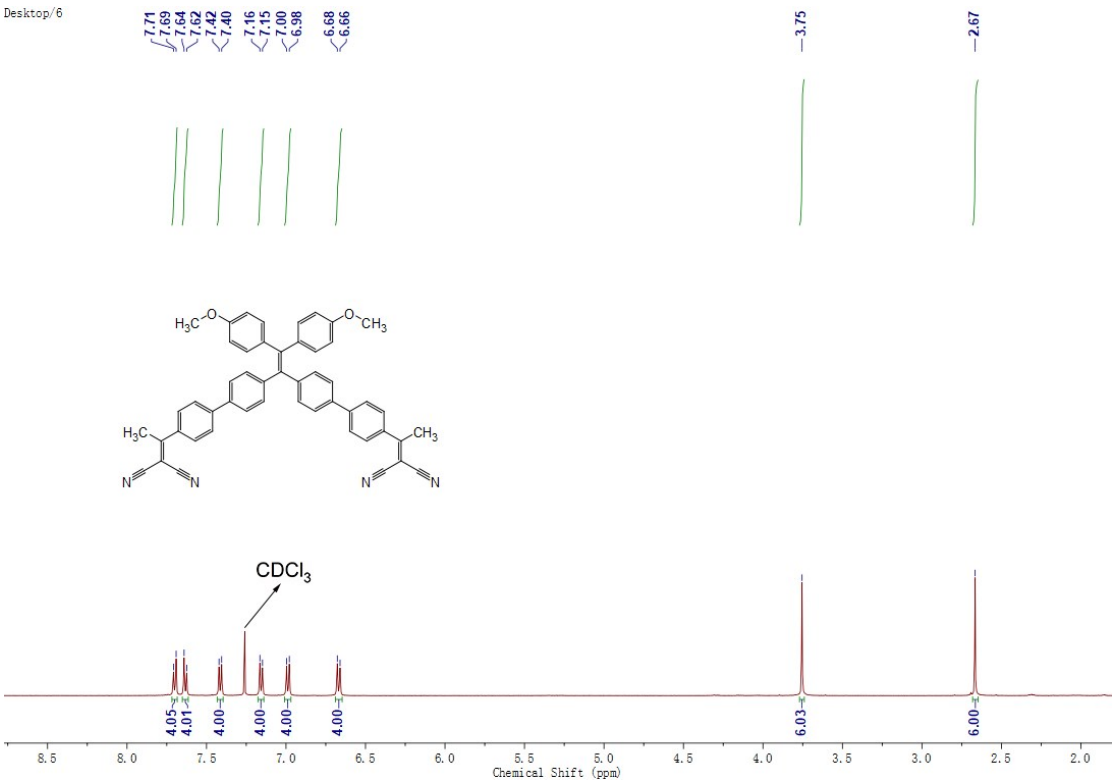

Figure S29. ^{1}H NMR spectrum of MTM in chloroform-d.

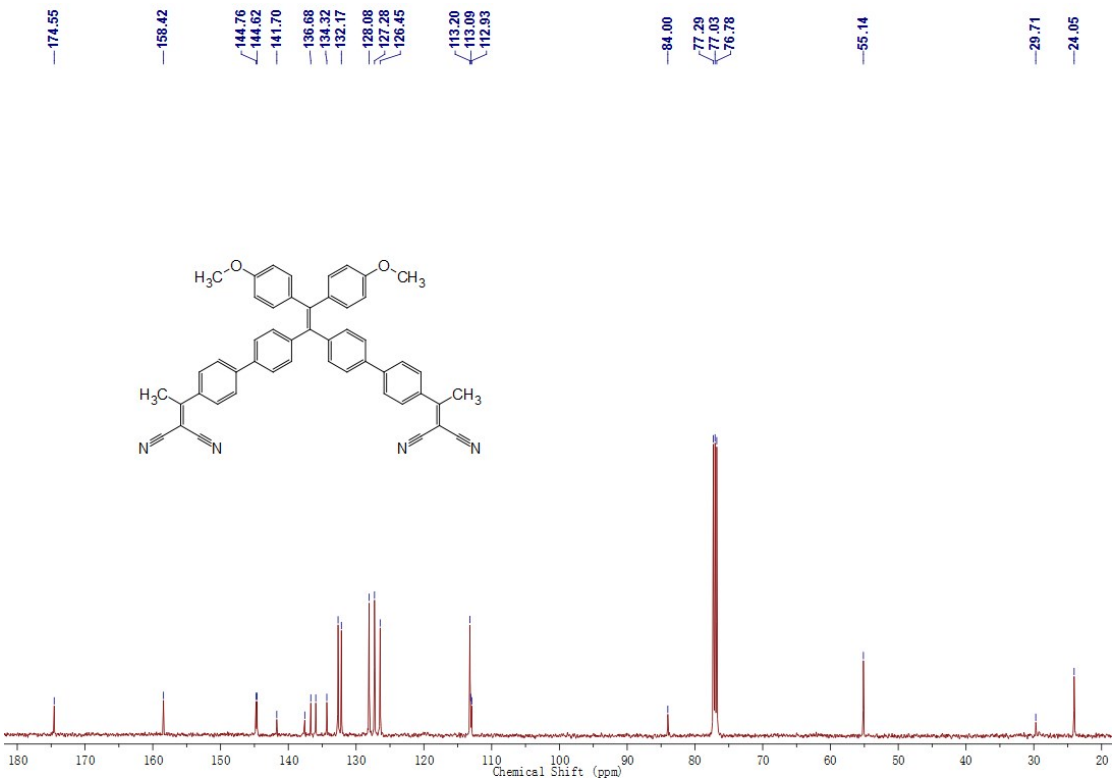

Figure S30. ^{13}C NMR spectrum of MTM in chloroform-d.

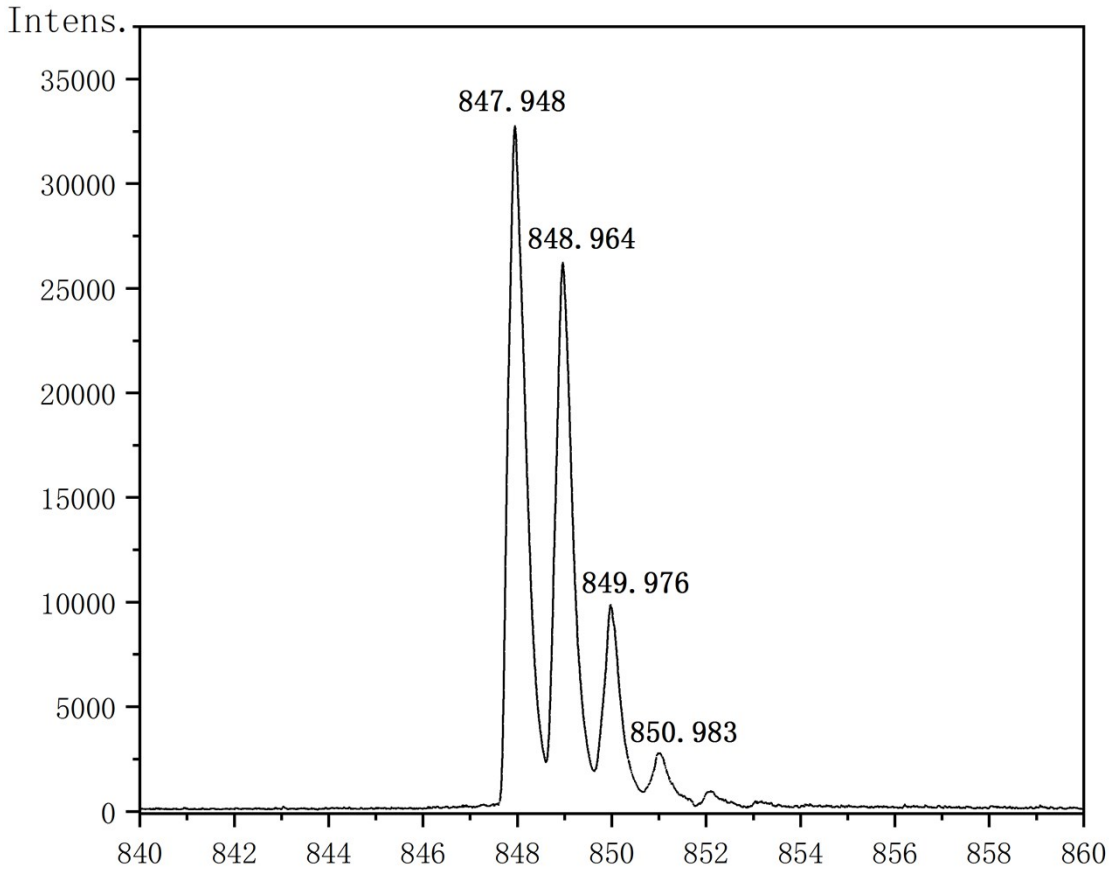

Figure S31. The MALDI-TOF mass spectrum of PTP.

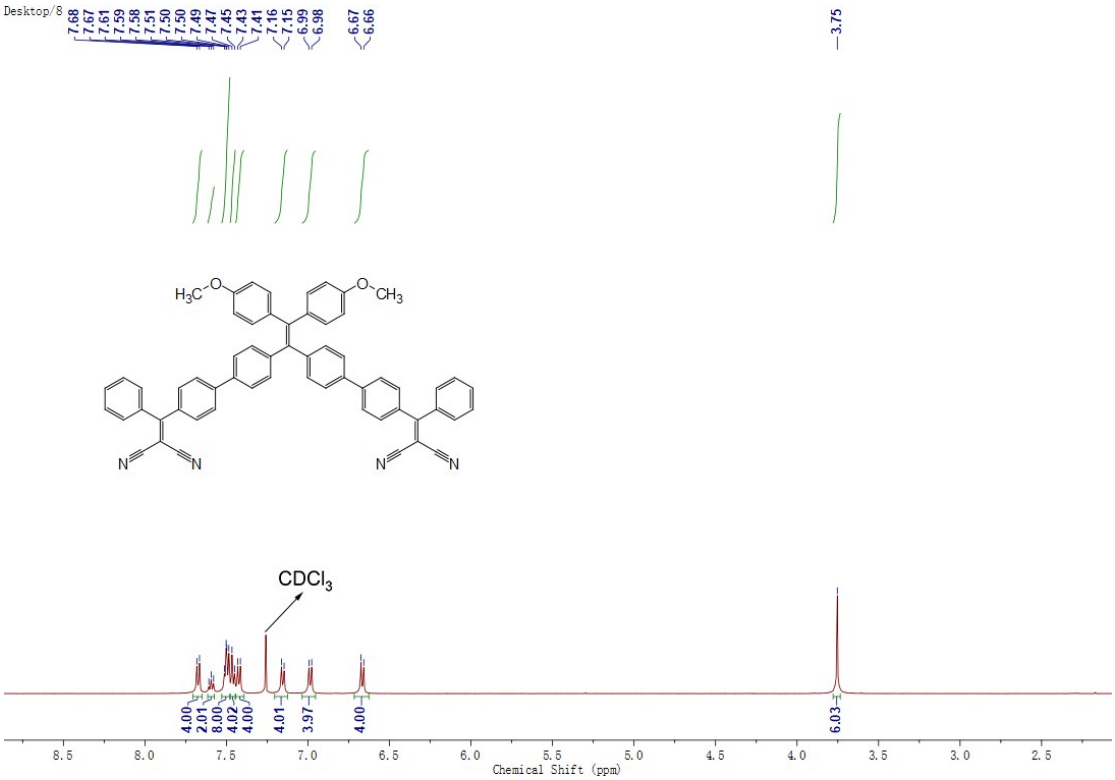

Figure S32. ^{1}H NMR spectrum of PTP in chloroform-d.

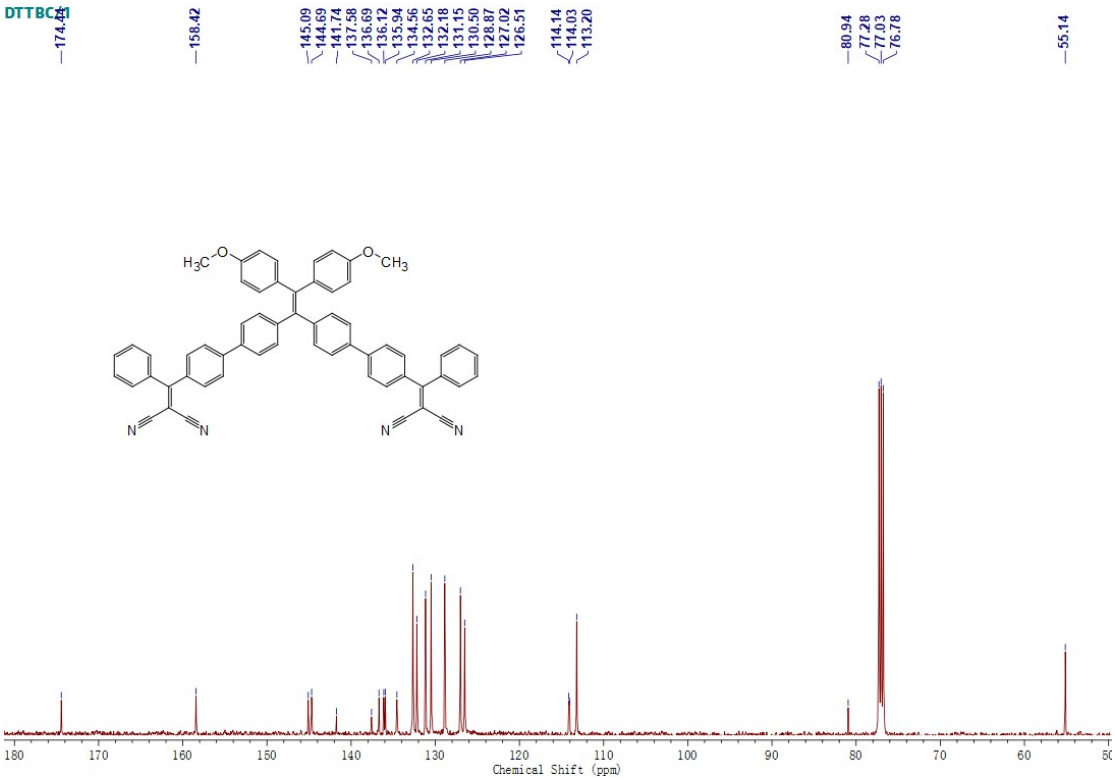

Figure S33. ^{13}C NMR spectrum of PTP in chloroform-d.

References

1. (a) S. D. Xu, W. B. Wu, X. L. Cai, C.-J. Zhang, Y. Y. Yuan, J. Liang, G. X. Feng, P. Manghnani, B. Liu, *Chem. Commun.*, 2017, **53**, 8727; (b) W. B. Wu, D. Mao, F. Hu, S. D. Xu, C. Chen, C.-J. Zhang, X. M. Cheng, Y. Y. Yuan, D. Ding, D. L. Kong, B. Liu, *Adv. Mater.*, 2017, **29**, 1700548.